

Extending the Coordination Chemistry of Molecular P_4S_3 : The Polymeric $Ag(P_4S_3)^+$ and $Ag(P_4S_3)_2^+$ Cations

Ariane Adolf,¹ Marcin Gonsior, and Ingo Krossing*

Contribution from Universität Karlsruhe, Institut für Anorganische Chemie, Engesserstrasse Geb. 30.45, D-76128 Karlsruhe, Germany

Received December 27, 2001

Abstract: Upon reacting P_4S_3 with $AgAl(hfip)_4$ and $AgAl(pftb)_4$ [$hfip = OC(H)(CF_3)_2$; $pftb = OC(CF_3)_3$], the compounds $Ag(P_4S_3)Al(hfip)_4$ **1** and $Ag(P_4S_3)_2^+[Al(pftb)_4]^-$ **2** formed in CS_2 (**1**) or CS_2/CH_2Cl_2 (**2**) solution. Compounds **1** and **2** were characterized by single-crystal X-ray structure determinations, Raman and solution NMR spectroscopy, and elemental analyses. One-dimensional chains of $[Ag(P_4S_3)_x]_{\infty}$ ($x = 1, 1; x = 2, 2$) formed in the solid state with P_4S_3 ligands that bridge through a 1,3-P,S, a 2,4-P,S, or a 3,4-P,P η^1 coordination to the silver ions. Compound **2** with the least basic anion contains the first homoleptic metal- (P_4S_3) complex. Compounds **1** and **2** also include the long sought sulfur coordination of P_4S_3 . Raman spectra of **1** and **2** were assigned on the basis of DFT calculations of related species. The influence of the silver coordination on the geometry of the P_4S_3 cage is discussed, additionally aided by DFT calculations. Consequences for the frequently observed degradation of the cage are suggested. An experimental silver ion affinity scale based on the solid-state structures of several weak Lewis acid base adducts of type $(L)AgAl(hfip)_4$ is given. The affinity of the ligand L to the silver ion increases according to $P_4 < CH_2Cl_2 < P_4S_3 < S_8 < 1,2-C_2H_4Cl_2 < toluene$.

Introduction

Recently, there has been a renewed interest in the coordination chemistry of small inorganic cage or ring molecules² such as P_4S_3 . However, the structural knowledge on intact coordinated P_4S_3 cages is limited to the apical η^1 -bound $Ni(np_3)_3$ and $Mo(CO)_5^4$ complexes. Very recently, the X-ray powder structures of two apical η^1 -bound BX_3 ($X = Br, I$) complexes of P_4S_3 were published.⁵ No further structurally characterized examples exist to the best of our knowledge.⁶ Normally, the P_4S_3 molecule degrades upon coordination to transition metal fragments, and phosphide and/or sulfide groups are incorporated into the complex.^{2,7} More recently, copper halide matrixes were shown to weakly coordinate intact phosphorus, phosphorus–selenium,

and chalcogen cages, rings, and chains.^{8,9} We obtained undistorted homoleptic P_4 and S_8 complexes with the even weaker Lewis acid Ag^+ ¹⁰ and the help of the very weakly coordinating anion (WCA) $Al(pftb)_4^-$ [$pftb = OC(CF_3)_3$],¹¹ that is, $Ag(\eta^2-P_4)_2^{+12}$ and $Ag(\eta^4-S_8)_2^{+13}$. In this work, our primary intent was to investigate the coordination behavior of undistorted P_4S_3 molecules with the naked Ag^+ ion. These weak complexes may be viewed as the primary steps of the usual degradation reactions of P_4S_3 ,^{2,7} and we were interested to learn about the most reactive coordination sites of this molecule with the simple Ag^+ ion as a nonsterically hindered model for a transition metal fragment (cf. Figure 1).

Results and Discussion

In contrast to the reactions of $AgAl(hfip)_4$ [$hfip = OC(H)(CF_3)_2$] and $AgAl(pftb)_4$ ¹¹ with P_4 ¹² or S_8 ,¹³ no isolated ions or molecules but in the solid-state polymeric silver- P_4S_3

* To whom correspondence should be addressed. Fax: ++49 721 608 48 54. E-mail: krossing@chemie.uni-karlsruhe.de.

- (1) A. Adolf prepared **1–2** in partial fulfillment of the advanced inorganic chemistry lab demonstration.
- (2) Reviews: (a) di Vaira, M.; Stoppioni, P. *Coord. Chem. Rev.* **1992**, *120*, 259. (b) Wachter, J. *Angew. Chem.* **1998**, *110*, 8782; *Angew. Chem., Int. Ed.* **1998**, *37*, 750. (c) Scherer, O. J. *Chem. Unserer Zeit* **2000**, *374*. (d) Whitmire, K. H. *Adv. Organomet. Chem.* **1998**, *42*, 2.
- (3) di Vaira, M.; Peruzzini, M.; Stoppioni, P. *Inorg. Chem.* **1983**, *22*, 2196.
- (4) Cordes, A. W.; Joyner, R. D.; Shores, R. D. *Inorg. Chem.* **1974**, *13*, 132.
- (5) Aubauer, C.; Irran, E.; Klapötke, T. M.; Schnick, W.; Schulz, A.; Senker, J. *Inorg. Chem.* **2001**, *40*, 4956.
- (6) However, the related $NbCl_5$ complexes of P_4S_4 and P_4Se_3 should be noted: Nowotnick, H.; Stumpf, K.; Blachnik, R. *Z. Anorg. Allg. Chem.* **1999**, *625*, 693. Additionally, P_4S_3 is very weakly bound in a supramolecular array within $(P_4S_3)[Ni(TMTAA)]$ with the shortest Ni– P_4S_3 distance at 3.22 Å: Andrews, P. C.; Atwood, J. L.; Barbour, L. J.; Nichols, P. J.; Raston, C. L. *Chem.-Eur. J.* **1998**, *4*, 1384.
- (7) See ref 2a for literature before 1992. New reports include: (a) Yoong Goh, L.; Chen, W.; Wong, R. C. S. *Angew. Chem.* **1993**, *105*, 1838. (b) Yoong Goh, L.; Chen, W.; Wong, R. C. S.; Karaghiosoff, K. *Organometallics* **1995**, *14*, 3886.

- (8) (a) Pfitzner, A.; Freudenthaler, E. *Angew. Chem.* **1995**, *107*, 1784; *Angew. Chem., Int. Ed. Engl.* **1995**, *34*, 1647. (b) Pfitzner, A.; Freudenthaler, E. *Z. Kristallogr.* **1995**, *210*, 59. (c) Pfitzner, A.; Freudenthaler, E. *Z. Kristallogr.* **1997**, *212*, 103. (d) Pfitzner, A.; Reiser, S.; Nilges, T. *Angew. Chem.* **2000**, *112*, 4328. (e) Pfitzner, A.; Reiser, S. *Inorg. Chem.* **1999**, *38*, 2451. (f) Pfitzner, A.; Nilges, T.; Deiseroth, H.-J. *Z. Anorg. Allg. Chem.* **1999**, *625*, 201. (g) Pfitzner, A.; Zimmerer, S. *Z. Anorg. Allg. Chem.* **1995**, *621*, 969.
- (9) Review: Pfitzner, A. *Chem.-Eur. J.* **2000**, *6*, 1891.
- (10) Because of the smaller radius but same unipositive charge, Cu^+ is a stronger Lewis acid than Ag^+ . Consistently, MS investigations showed the binding energies of $Cu^+(L)$ complexes in the gas phase to be higher by 30 to 50 kJ mol⁻¹ if compared to the respective $Ag^+(L)$ species, that is, $L = C_2H_4, CO, C_6H_6$, etc.
- (11) Krossing, I. *Chem.-Eur. J.* **2001**, *7*, 490.
- (12) (a) Krossing, I. *J. Am. Chem. Soc.* **2001**, *123*, 4603. (b) Krossing, I.; van Wüllen, L. *Chem.-Eur. J.* **2002**, *8*, 500.
- (13) Krossing, I.; Cameron, T. S.; Decken, A.; Dionne, I.; Fang, M.; Passmore, J. *Chem.-Eur. J.*, in press.

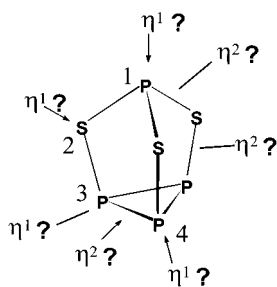
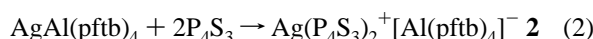
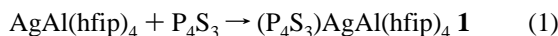


Figure 1. Possible coordination sites of the C_{3v} symmetric P_4S_3 molecule.

complexes $(P_4S_3)AgAl(hfip)_4$ **1**¹⁴ and $[Ag(P_4S_3)_2]^+[Al(pftb)_4]^-$ **2**¹⁵ formed from CS_2 (**1**) and CS_2/CH_2Cl_2 (10:1, **2**) solution (eqs 1 and 2).



Compounds **1** and **2** are highly soluble in CH_2Cl_2 and CS_2/CH_2Cl_2 mixtures, and therefore it is likely that dissolved **1** adopts an isolated molecular structure as in $(L)AgAl(hfip)_4$ and dissolved **2** adopts a structure with discrete isolated ions as in $Ag(L)_2^+[Al(pftb)_4]^-$ ($L = P_4[12b]; S_8^{13}$). The variable temperature (VT) ^{31}P NMR spectra of **1** and **2** in CD_2Cl_2 are nearly unchanged if compared to P_4S_3 in the same solvent ($\Delta\delta = 2$ – 10 ppm) and indicate exchange reactions and a weak bonding to the silver ion. However, the ready observation of a ^{31}P solution NMR spectrum at -90 °C showed that the signals are due to **1** and **2** and not to free P_4S_3 which is insoluble in CH_2Cl_2 at -90 °C. Similar to **1** and **2**, the position of the ^{31}P NMR shift of the related silver-P₄ adducts was only very slightly changed if compared to free P_4 ¹⁶ and in solid $P_4S_3 \cdot BX_3$ $\Delta(\delta^{31}P)$ was 5–57 ppm.⁵ Also the $^2J_{PP}$ coupling constants in **1** and **2** are only slightly changed by $\Delta(^2J_{PP}) = 1$ –6 Hz if compared to free P_4S_3 in the same solvent (69 Hz). Compounds **1** and **2** are stable for at least several hours in daylight but highly sensitive toward

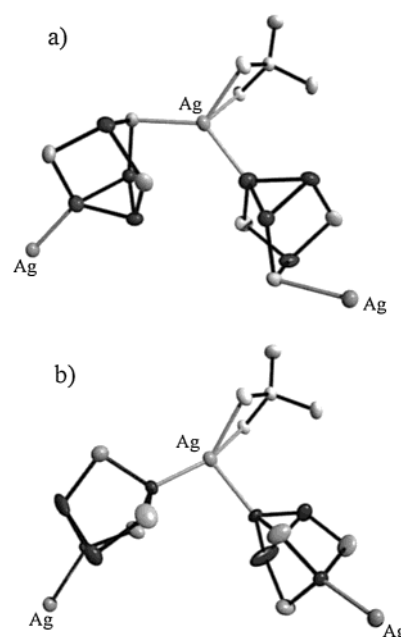


Figure 2. The solid-state structure of the polymeric $Ag(P_4S_3)$ moiety in **1** at 170 K. (a) This denotes the structure occupied by 68.6% of the P_4S_3 molecules in **1a**, (b) and that occupied by 31.4% in **1b**. The $C(H)(CF_3)_2$ ligands of the $Al(hfip)_4^-$ anion were omitted for clarity. The bonds within the AlO_4 unit and the P_4S_3 cage were drawn in black, those to the silver ion in gray. The Ag atoms completing the coordination on the left and right are also shown. Thermal ellipsoids were drawn at the 25% probability level, P atoms are shown in black, S atoms in light gray, Ag atoms in medium gray, and Al, O in white.

oxygen, and crystals exposed to the atmosphere turn brownish-black within less than a second. The solid-state structures¹⁷ of **1** and **2** contain one-dimensional infinite chains that are built from tetracoordinate Ag^+ ions and one or two bridging P_4S_3 molecules. In **1**, the P_4S_3 molecules adopt two independent positions with a 68.6 (=1a) and 31.4% (=1b) occupation each.¹⁸ All η^1 bonding modes shown in Figure 1 are realized in **1** and **2**, but no η^2 -P,S or η^2 -P,P coordination as in the $Ag(\eta^2-P_4)$ complexes¹² was observed. In **1** (Figure 2) with the more basic anion two of the four silver coordination sites are occupied by the oxygen atoms of the $Al(hfip)_4^-$ anion at 2.435(4) and 2.455(4) Å as in (molecular) $(L)AgAl(hfip)_4$ $d(Ag-O) = 2.345(3)$ – $2.737(3)$ Å ($L = P_4[12b]; S_8^{13}$). In contrast, **2** (Figure 3) with the less basic anion¹¹ has no silver-anion contacts below 4.0 Å, and to complete the coordination environment the silver ion coordinates a second P_4S_3 molecule as in (monomeric)

(14) Synthesis of **1**: Solid $AgAl(hfip)_4$ (1.004 g, 1.25 mmol) and solid P_4S_3 (0.275 g, 1.25 mmol) were weighed into a Schlenk vessel. CS_2 (10 mL) was added at room temperature, and the mixture was stirred overnight after which a colorless solution over a smaller amount of dark brownish precipitate had formed. The suspension was filtered, and the filtrate was concentrated to about 5 mL and stored overnight in a -30 °C freezer. Large, colorless, very air- and moisture-sensitive, blocklike crystals of **1** formed and were isolated (0.981 g, 77% yield). mp 128–139 °C. Raman data are given in Table 2. 1H NMR (250 MHz, CD_2Cl_2 , 25 °C): $\delta = 4.55$ (sept., $^3J_{HF} = 5.6$ Hz). ^{13}C NMR (63 MHz, CD_2Cl_2 , 25 °C): $\delta = 71.1$ (sept., $^2J_{CF} = 33.0$ Hz), 122.7 (q, CF_3 , $^1J_{CF} = 286.1$ Hz). ^{27}Al NMR (78 MHz, CD_2Cl_2 , 25 °C): $\delta = 60.1$ (s, $\nu_{1/2} = 280$ Hz). ^{31}P NMR (101 MHz, CD_2Cl_2 , 25 °C): $\delta = 66.8$ (q, P_{apical} , $^2J_{PP} = 62.7$ Hz), -126.5 (d, P_{basal} , $^2J_{PP} = 62.7$ Hz). ^{31}P NMR (101 MHz, CD_2Cl_2 , -90 °C): $\delta = 72.7$ (s, P_{apical} , $\nu_{1/2} = 226$ Hz), -118.2 (s, P_{basal} , $\nu_{1/2} = 339$ Hz). Anal. Calcd for $C_{12}H_4Ag_1Al_1F_{24}O_9P_4S_3$: Ag, 10.5; C, 14.09. Found: Ag, 9.6; C, 13.72.

(15) Synthesis of **2**: Solid $Ag(CH_2Cl_2)Al(pftb)_4$ (0.411 g, 0.35 mmol) and solid P_4S_3 (0.150 g, 0.70 mmol) were weighed into a two bulb vessel incorporating a fine sintered glass frit and two J. Young valves. CS_2 (10 mL) and CH_2Cl_2 (1 mL) were added at room temperature, and the mixture was stirred overnight after which a colorless solution over a smaller amount of dark brownish precipitate had formed. The suspension was filtered, and the filtrate was concentrated until it had an oily consistency with very little solvent left. This oil was left overnight in a 0 °C freezer after which the oil quantitatively had crystallized. The remaining few drops of solvent were decanted, and the needle-shaped colorless crystals of **2** dried in a dynamic vacuum (0.48 g, 90% yield). Raman data are given in Table 2. ^{13}C NMR (63 MHz, CD_2Cl_2 , 25 °C): $\delta = 121.5$ (q, CF_3 , $^1J_{CF} = 293.1$ Hz). ^{27}Al NMR (78 MHz, CD_2Cl_2 , 25 °C): $\delta = 36.0$ (s, $\nu_{1/2} = 12$ Hz). ^{31}P NMR (101 MHz, CD_2Cl_2 , 25 °C): $\delta = 72.2$ (q, P_{apical} , $^2J_{PP} = 68.1$ Hz), -118.8 (d, P_{basal} , $^2J_{PP} = 67.9$ Hz). ^{31}P NMR (101 MHz, CD_2Cl_2 , -90 °C): $\delta = 78.7$ (s, P_{apical} , $\nu_{1/2} = 174$ Hz), -109.1 (s, P_{basal} , $\nu_{1/2} = 201$ Hz). Anal. Calcd for $C_{16}Ag_1Al_1F_{36}O_9P_8S_6$: C, 12.68. Found: C, 12.19.

(16) Additionally established by VT ^{31}P -MAS NMR spectra of $Ag(P_4)_2^+[Al(pftb)_4]^-$.¹²

(17) Crystal structure determination of **1** [2]: IPDS (Stoe), graphite monochromated Mo K α radiation, $T = 175(2)$ [2, 150(2)] K, unit cell determination, 5000 reflections, corrections, Lorentz, Polarisation, and numerical absorption correction, $\mu = 1.215$ [2, 1.244] cm^{-1} , direct methods with SHELXS-97, refinement against F^2 with SHELXL-97. Data for **1**: space group, $P2_1/n$, $Z = 4$, $a = 16.680(3)$, $b = 11.185(2)$, $c = 18.324(4)$ Å, $\beta = 110.38(3)^\circ$, $V = 3204.6(11)$ Å³, $\rho_{calcd} = 2.120$ $g\ cm^{-3}$, $2\theta_{max} = 52^\circ$, reflections, 16 899 collected, 5335 unique, 4144 observed (4σ), $R_{int} = 0.0538$, 506 parameter, 13 SADI restraints (to fix the anion), $R_1 = 0.0504$, wR_2 (all data) = 0.1444, GOF = 1.033. Data for **2**: space group, $P2_1/n$, $Z = 4$, $a = 16.3639(14)$, $b = 10.9494(5)$, $c = 26.470(2)$ Å, $\beta = 94.578(10)^\circ$, $V = 4727.7(6)$ Å³, $\rho_{calcd} = 2.236$ $g\ cm^{-3}$, $2\theta_{max} = 52^\circ$, reflections, 14 790 collected, 7135 unique, 6002 observed (4σ), $R_{int} = 0.0262$, 742 parameter, $R_1 = 0.0435$, wR_2 (all data) = 0.1175, GOF = 1.058. The structure contains one non-interacting cocrystallized CS_2 molecule disordered over two positions in a 75:25 ratio.

(18) The bond distances of the less populated 31.4% site have larger standard deviations of 0.01–0.02 Å, and the position of the atoms is not as well resolved as in the main occupation. Therefore, a structural discussion of this geometry (Figure 1b) is omitted. However, a second data set of a crystal of **1** synthesized in an independent preparation gave very similar structural data (within 0.01 Å), and the ratio between the two isomers was 60% versus 40%.

Table 1. Comparison of the Structural Parameter of Free and Coordinated P_4S_3 Molecules

parameter	$\text{P}_4\text{S}_3^{24}$	$\mathbf{1a}^{18}$	$\mathbf{2}$	$(\text{np}^3)\text{Ni}(\text{P}_4\text{S}_3)^3$
$d(\text{Ag}-\text{P})_{\text{range}}$		2.523(4)	2.512(1)–2.540(1)	
$d(\text{Ag}-\text{P})_{\text{av}}$			2.529	
$d(\text{Ag}-\text{S})$		2.571(2)	2.657(1)	
$d(\text{P}-\text{P})_{\text{range}}$	2.223(1)–2.235(1)	2.197(5)–2.295(5)	2.217(1)–2.256(1)	<i>a</i>
$d(\text{P}-\text{P})_{\text{av}}$	2.227	2.257	2.237	2.223(7)
$d(\text{P}_{\text{apical}}-\text{S})_{\text{range}}$	2.089(1)–2.098(1)	2.139(4)–2.189(4)	2.094(1)–2.134(1)	<i>a</i>
$d(\text{P}_{\text{apical}}-\text{S})_{\text{av}}$	2.092	2.158	2.112	2.129(4)
$d(\text{P}_{\text{basal}}-\text{S})_{\text{range}}$	2.087(1)–2.089(1)	1.959(4)–2.146(4)	2.069(1)–2.110(1)	<i>a</i>
$d(\text{P}_{\text{basal}}-\text{S})_{\text{av}}$	2.086	2.071	2.083	2.090(5)

^a Three-fold symmetry in the crystal, therefore no range.

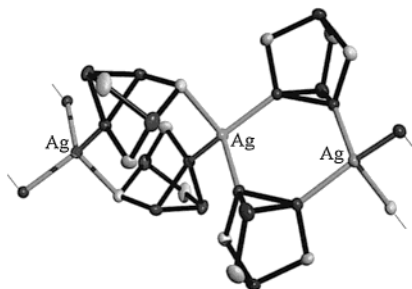


Figure 3. The solid-state structure of the polymeric homoleptic $\text{Ag}(\text{P}_4\text{S}_3)_2^{2+}$ cation in $\mathbf{2}$ at 150 K. One complete repetitive $[\text{Ag}(\text{P}_4\text{S}_3)_2]_2$ unit of the infinite chain of $[\text{Ag}(\text{P}_4\text{S}_3)_2]_\infty$ containing six-membered planar Ag_2P_4 and eight-membered slightly puckered $\text{Ag}_2\text{P}_4\text{S}_2$ rings is shown. The bonds within the P_4S_3 cage were drawn in black, those to the silver ion in gray. The P and S atoms completing the coordination of the left and right Ag atoms are also shown. Thermal ellipsoids were drawn at the 25% probability level, P atoms are shown in black, S atoms in light gray, and Ag atoms in medium gray. The $\text{Al}(\text{pftb})_4^-$ anion was omitted for clarity.

$\text{Ag}(\text{L})_2^+[\text{Al}(\text{pftb})_4^-]$ ($\text{L} = \text{P}_4^{12b}$; S_8^{13}). (Full ellipsoid plots of $\mathbf{1}$ and $\mathbf{2}$ with distances and angles are deposited.)

The P_4S_3 molecules bridge to the Ag^+ ions through a 1,3-P,P ($\mathbf{1b}$), a 2,4-P,S ($\mathbf{1a}$, $\mathbf{2}$), or a 3,4-P,P ($\mathbf{2}$) coordination (labeling as in Figure 1). Planar six- and slightly puckered eight-membered rings formed in $\mathbf{2}$ (Figure 3). Similar planar M_2P_4 rings were earlier found by Scheer et al. ($\text{M} = \text{Mo}$)¹⁹ and Scherer et al. ($\text{M} = \text{Re}$)²⁰. The 1,3 or 2,4 coordination in $\mathbf{1}$ and $\mathbf{2}$ is similar to the 1,3 coordination of the S_8 molecule in $(\text{S}_8)_2\text{-AgAsF}_6$ ²¹ or polymeric $(\text{S}_8)\text{Rh}_2(\text{O}_2\text{CCF}_3)_4$.²² The $\text{Ag}-\text{P}$ distance in $\mathbf{1a}^{18}$ is 2.523(4) Å; in $\mathbf{2}$ they are 2.540(1), 2.534(1) (six-ring), and 2.512(1) Å (eight-ring) – similar to the $\text{Ag}-\text{P}$ distances in the $\text{Ag}(\eta^2\text{-P}_4)$ adducts of 2.512–2.548 Å.¹² $\text{Ag}-\text{S}$ bond lengths range from 2.571(2) in $\mathbf{1a}$ to 2.657(1) in $\mathbf{2}$ (eight-ring) and are comparable to those of the $\text{Ag}(\text{S}_8)$ adducts as in $(\text{S}_8)_2\text{AgAsF}_6$ ²¹ (2.724 and 2.802 Å) or $[\text{Ag}(\text{S}_8)_2^+][\text{Al}(\text{pftb})_4^-]$ (2.622, 2.794, 2.838 Å).¹³ Surprisingly, both $\text{Ag}-\text{P}$ and $\text{Ag}-\text{S}$ distances are similar to the values found in the solid binaries Ag_2S and Ag_3P_{11} containing the charged and, therefore, seemingly more basic S^{2-} and P_{11}^{3-} anions.²³ However, similar observations were made frequently for the distances of Ag^+/Cu^+ to neighboring neutral or anionic arrangements.^{8,9} The

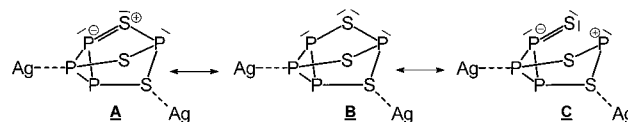


Figure 4. Selected VB structures that possibly account for the short and/or long adjacent P–S distances in $\mathbf{1a}$. Other possible VB structures are presumably of less weight and were therefore omitted.

structural parameters of the coordinated P_4S_3 molecules in $\mathbf{1}$ are more affected by the coordination than those observed in $\mathbf{2}$; that is, P–P [P–S] bonds in $\mathbf{1a}^{18}$ range from 2.197(5) to 2.295(5) [1.959(4) to 2.189(4)] Å and in $\mathbf{2}$ from 2.217(1) to 2.256(1) [2.071(1) to 2.134(1)] Å. The average distances in $\mathbf{1}$ and $\mathbf{2}$ compare well to those observed in free P_4S_3 ²⁴ and coordinated $(\text{np}^3)\text{Ni}(\text{P}_4\text{S}_3)^3$ (see Table 1).

As seen from Table 1, P–S or P–P bonds in $\mathbf{1}$ and $\mathbf{2}$ are shortened or elongated by up to +0.10/–0.13 Å if compared to free P_4S_3 . The shortest P–S bond length of 1.959(4) Å in $\mathbf{1a}^{25}$ is close to a P=S double bond; that is, $d(\text{P}=\text{S}_{\text{exo}})$ in P_4S_{10} is 1.91 Å.²⁶ This short P–S bond is accompanied by an adjacent very long P–S bond of 2.189(4) Å. Figure 4 gives selected possible VB structures that may be responsible for this phenomenon.

In agreement with the DFT calculations below, VB structures **A** and **C** possibly account for the short P–S bond and **C** for the long adjacent P–S distance. Other possible VB structures (not shown) appear to be of less weight.

To understand the bonding within the $\text{Ag}(\text{P}_4\text{S}_3)$ adducts, to verify the two geometries found in $\mathbf{1ab}$, to compare the six- and eight-ring in $\mathbf{2}$, as well as to calculate the vibrational frequencies of these species to aid the assignment of the experimental Raman frequencies of $\mathbf{1}$ and $\mathbf{2}$, we fully optimized P_4S_3 (C_{3v}), two isomers of $\text{Ag}_2\text{P}_4\text{S}_3^{2+}$ (C_1) as included in $\mathbf{1ab}$, and the six- (C_{2h}) and eight-ring (C_i) ($\text{AgP}_4\text{S}_3)_2^{2+}$ as found as part of $\mathbf{2}$ at the (RI-)BP86/SVP (DFT-)level.^{27–30} All optimized geometries shown in Figure 5 are in good qualitative agreement with the experimental structures and are true minima with no

(24) Gruber, H.; Müller, U. Z. *Kristallogr.* **1997**, *202*, 662.

(25) This distance may also be affected by the disorder¹⁸ and therefore could be longer. However, this is not reflected in the standard deviation or the ellipsoid plot of the P_4S_3 cage in $\mathbf{1a}$.

(26) Greenwood, N. N.; Eamshaw, A. *Chemistry of the Elements*, 2nd ed.; Butterworth-Heinemann: Oxford, 1997.

(27) All computations were done with the program TURBOMOLE.²⁸ The geometries of all species were optimized at the (RI-)BP86 (DFT) level²⁹ with the split valence polarisation SVP basis set.³⁰ The 28 core electrons of Ag were replaced by a quasi relativistic effective core potential. Frequency calculations were performed at the BP86/SVP level, and all structures represent true minima without imaginary frequencies on the respective hypersurface. In Table 2, only the Raman active vibrational modes of the 6 ring and the 8 ring ($\text{AgP}_4\text{S}_3)_2^{2+}$ are given. Full vibrational frequencies of all ($\text{AgP}_4\text{S}_3)_2^{2+}$ species are provided in the Supporting Information. For selected species, a modified Roby–Davidson population analysis has been performed using the BP/SVP electron density.

(19) Sekal, P.; Umbarkar, S.; Scheer, M.; Voigt, A.; Kirmse, R. *Eur. J. Inorg. Chem.* **2000**, 2585.

(20) Scherer, O. J.; Sitzmann, H.; Wolmershäuser, G. *Angew. Chem.* **1984**, *96*, 979; *Angew. Chem., Int. Ed. Engl.* **1984**, *23*, 931.

(21) Roesky, H. W.; Thomas, M.; Schimkowiak, J.; Jones, P. G.; Pinkert, W.; Sheldrick, G. M. *J. Chem. Soc., Chem. Commun.* **1982**, 895. (b) Roesky, H. W.; Witt, M. *Inorg. Synth.* **1986**, *24*, 72.

(22) Cotton, F. A.; Dikarev, E. V.; Petrukhina, M. A. *Angew. Chem.* **2001**, *113*, 1569.

(23) (a) Moeller, M.; Jeitschko, W. *Z. Anorg. Allg. Chem.* **1982**, *491*, 225. (b) Moeller, M.; Jeitschko, W. *Inorg. Chem.* **1981**, *20*, 828. (c) Cava, R. J.; Reidinger, F.; Wuensch, B. J. *J. Solid State Chem.* **1980**, *31*, 69.

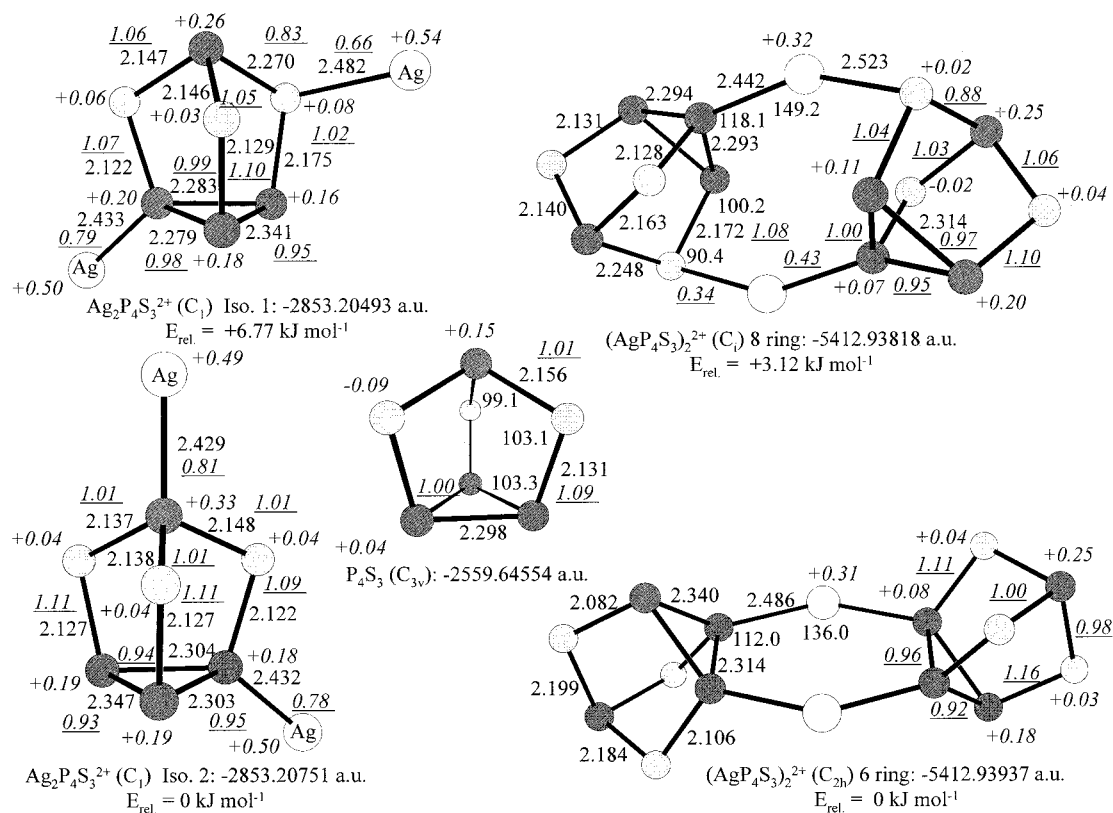


Figure 5. BP86/SVP optimized structures, total and relative energies of P_4S_3 , as well as two isomers of $\text{Ag}_2\text{P}_4\text{S}_3^{2+}$ and $(\text{AgP}_4\text{S}_3)_2^{2+}$ as observed as parts of the polymeric solid-state structures of **1** and **2**. Distances are given in Å and bond angles in deg. Computed partial charges are given in italics and shared electron numbers in italics and underlined.

imaginary frequencies. All bond lengths are overestimated by about 0.05–0.10 Å as frequently found with DFT.^{31,32}

A large range of the P–S bond lengths similar to that in the experiment was found in the calculation, and the shared electron numbers (SENs) of the P–S bonds range from 0.83 to 1.16 but only 1.01 to 1.09 in free P_4S_3 . This supports the importance of the proposed VB structures A and C in Figure 3 above. Both sets of isomers in Figure 5 are almost isoenergetic, and their relative energies differ only by 6.77 kJ mol⁻¹ ($\text{Ag}_2\text{P}_4\text{S}_3^{2+}$) or 3.12 kJ mol⁻¹ [$(\text{AgP}_4\text{S}_3)_2^{2+}$]. With these small energetic differences, it is easy to understand that two different coordination modes are found in the solid-state structures of **1** and **2**. From the calculated partial charges and SENs it is evident that (i) the Ag–P and Ag–S interactions have covalent contributions and therefore SENs ranging from 0.34 to 0.81 and (ii) the positive charges are delocalized over the entire species with higher partial charges residing on Ag (+0.31 to +0.54) and P (+0.07 to +0.33), but the sulfur atoms are almost uncharged (–0.02 to +0.08). If the Ag– P_4S_3 bonding would be purely electrostatic, one would expect a preference for the formation of Ag–S bonds since the sulfur atoms in free P_4S_3 are negatively

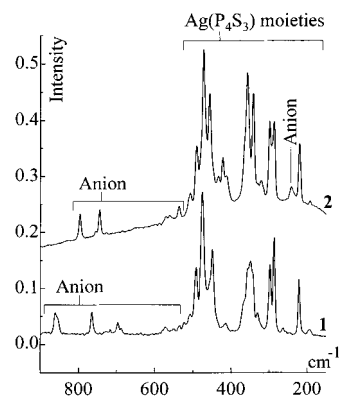


Figure 6. FT-Raman spectra of **1** (bottom trace) and **2** (top trace) between 100 and 900 cm⁻¹.

polarized (–0.09, Figure 5), and, on electrostatic grounds, bonds to sulfur should be favored.

The Raman spectra of **1** and **2**, shown in Figure 6, and free P_4S_3 are compared in Table 2. Bands of the anions and the coordinated P_4S_3 molecules are visible in Figure 6. Because of the lowering of the symmetry upon silver coordination, several degenerate or Raman forbidden modes split in C_{3v} - P_4S_3 and are visible in **1** and **2**. The frequencies of the anions are listed in a deposited section. Assignments were made on the basis of those reported for the free P_4S_3 molecule³³ and the calculated BP86/SVP frequencies of $\text{Ag}_2\text{P}_4\text{S}_3^{2+}$ and $(\text{AgP}_4\text{S}_3)_2^{2+}$.

The vibrational frequencies of the coordinated P_4S_3 molecules in **1** and **2** versus those of free P_4S_3 are changed by a maximum

- (28) TURBOMOLE, Version 5: (a) Ahlrichs, R.; Bär, M.; Häser, M.; Horn, H.; Kölmel, C. *Chem. Phys. Lett.* **1989**, *162*, 165. (b) Arnim, M. v.; Ahlrichs, R. *J. Chem. Phys.* **1999**, *111*, 9183.
- (29) Weigend, F.; Häser, M. *Theor. Chim. Acta* **1997**, *97*, 331.
- (30) (a) Schäfer, A.; Horn, H.; Ahlrichs, R. *J. Chem. Phys.* **1992**, *97*, 2571. (b) Schäfer, A.; Huber, C.; Ahlrichs, R. *J. Chem. Phys.* **1994**, *100*, 5829.
- (31) (a) Jenkins, H. D. B.; Jitariu, L. C.; Krossing, I.; Passmore, J.; Suontamo, R. *J. Comput. Chem.* **2000**, *21*, 218. (b) Krossing, I.; Passmore, J. *Inorg. Chem.* **1999**, *38*, 5203. (c) Cameron, T. S.; Deeth, R. J.; Dionne, I.; Jenkins, H. D. B.; Krossing, I.; Passmore, J.; Roobottom, H. *Inorg. Chem.* **2000**, *39*, 5614.
- (32) Koch, W.; Holtshausen, M. C. *A Chemists Guide to Density Functional Theory*, 1st ed.; Wiley-VCH: Weinheim, 2000.

- (33) Bues, W.; Somer, M.; Brockner, W. *Z. Naturforsch.* **1980**, *35b*, 1063.

Table 2. Experimental Room Temperature Raman Spectra of P_4S_3 , **1**, and **2** on Our Spectrometer (1064 nm Radiation, 2 cm^{-1} Resolution) [in cm^{-1}]^a

assign. and sym. for P_4S_3 ³³	P_4S_3 exp (%)	P_4S_3 calc ^b sy	1 exp (%)	iso 1 calc ^b	iso 2 calc ^b	2 exp (%)	six-ring RA calc ^b (sy)	eight-ring RA calc ^b (sy)
$\nu(\text{P}_3) \text{A}_1 + \nu(\text{P}_{\text{apical}}-\text{S}_3) \text{E}$	487 (18)	463 E	507 (13) 491 (47)	485	492	507 (15) 490 (43)	501 B _g 495 A _g	
		447 A ₁	475 (100) 455 (sh)	453	478	472 (100)	468 A _g	473 A _g
$\nu(\text{P}_{\text{basal}}-\text{S}) \text{A}_1$	441 (100)	428 A ₁	449 (58) 414 (9)	444 409	437 410 (2x)	456 (72) 433 (23)	441 A _g	452 A _g 439 A _g
$\nu(\text{P}_{\text{apical}}-\text{S}_3) \text{A}_1$	420 (19)	387 A ₁		397	400	422 (34)		415 A _g
$\nu(\text{P}_{\text{basal}}-\text{S}) \text{E}$	417 (sh)	389 E		390		408 (22)		392 A _g 385 A _g
			367 (sh)			361 (sh)	369 A _g 368 B _g 361 A _g 357 B _g	
			356 (51, b)		357	357 (83) 354 (sh)		
$\nu(\text{P}_3) \text{E}$	341 (52)	323 E	349 (57, b)	345		342 (54)		347 A _g
			344 (sh)	339		326 (5)	330 A _g 326 A _g	332 A _g 327 A _g 311 A _g
			298 (47) 287 (60)	302 285		299 (51) 287 (51)	293 B _g 286 A _g	291 A _g 273 A _g 265 A _g
$\delta(\text{P}_{\text{apical}}-\text{S}_3) \text{A}_1$	285 (23)	287 E	263 (5) 254 (2)	278 249	285 267			
					214		207 B _g	
$\delta(\text{P}_{\text{basal}}-\text{S}) \text{E}$	220(9)	219 E	221 (32)	212	209	220 (35)	205 A _g	211 A _g
$\delta(\text{P}_{\text{apical}}-\text{S}_3) \text{E}$	182 (2)	190 A ₂	193 (5) 120 (7) 86 (1)	186 129 99	177 127 75	192 (3)	184 B _g	187 A _g

^a b = broad. For comparison, the BP86/SVP calculated vibrational frequencies of $\text{Ag}_2\text{P}_4\text{S}_3^{2+}$ (**iso 1** and **iso 2**) and $(\text{AgP}_4\text{S}_3)_2^{2+}$ (six- and eight-ring) are included. Only the Raman active (RA) frequencies of $(\text{AgP}_4\text{S}_3)_2^{2+}$ are included (the others are deposited). ^b BP86/SVP.

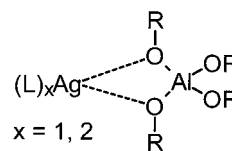
Table 3. Ag–O Distances [in \AA] and Ag–O Bond Valences s [in vu] of Several Lewis Acid Base Adducts $(\text{L})\text{AgAl}(\text{hftp})_4$ and $(\text{L})\text{AgAl}(\text{hftb})_4$ [$\text{hftb} = \text{OC}(\text{CH}_3)(\text{CF}_3)_2$]^a

$\text{Ag}(\text{tol})_2\text{-Al}(\text{hftp})_4$ ¹¹		$\text{Ag}(\text{Di})_2\text{-Al}(\text{hftp})_4$ ¹¹		$\text{Ag}(\text{S}_8)\text{-Al}(\text{hftp})_4$ ¹³		$\text{Ag}(\text{P}_4)\text{-Al}(\text{hftp})_4$		$\text{Ag}(\text{CH}_2\text{Cl}_2)\text{-Al}(\text{hftb})_4$ ¹¹		$\text{Ag}(\text{P}_4)\text{-Al}(\text{hftb})_4$ ^{12b}		$\text{Ag}(\text{P}_4)\text{-Al}(\text{hftp})_4$ ^{12b}	
$d(\text{Ag}-\text{O})$	vu	$d(\text{Ag}-\text{O})$	vu	$d(\text{Ag}-\text{O})$	vu	$d(\text{Ag}-\text{O})$	vu	$d(\text{Ag}-\text{O})$	vu	$d(\text{Ag}-\text{O})$	vu	$d(\text{Ag}-\text{O})$	vu
2.596	0.119	2.492	0.160	2.345	0.252	2.435	0.190	2.377	0.228	2.365	0.236	2.353	0.245
2.599	0.118	2.576	0.126	2.737	0.080	2.455	0.179	2.386	0.221	2.388	0.220	2.401	0.211
sum vu	0.236	sum vu	0.286	sum vu	0.332	sum vu	0.370	sum vu	0.449	sum vu	0.456	sum vu	0.457

^a Di = 1,2- $\text{Cl}_2\text{C}_2\text{H}_4$, tol = toluene.

of about 30 cm^{-1} . By comparison to the calculated frequencies of the $\text{Ag}_2\text{P}_4\text{S}_3^{2+}$ and $(\text{AgP}_4\text{S}_3)_2^{2+}$ isomers in Table 2, it is evident that each of the two different isomers included in the solid-state structures of **1** and **2** gives a distinct Raman spectrum that is separated from each other (Table 2). The highest energy bands $\nu(\text{P}_{\text{apical}}-\text{S}_3)$ (E) of the coordinated P_4S_3 molecules are found 20 cm^{-1} higher in energy than those in free P_4S_3 . This is in agreement with the solid-state structures of **1** and **2**, where at least one apical P–S bond is shorter, and therefore stronger, by 0.127^{25} (**1a**) to 0.018 (**2**), \AA , as in free P_4S_3 .

An Experimental Silver Ion Affinity Scale. Silver ion affinity (SIA) scales were previously established in the gas phase by mass spectrometry³⁴ and computational chemistry.³⁵ However, to the best of our knowledge, no attempt has been made to obtain a SIA scale based on solid-state structures. Recently, we structurally characterized several Lewis acid base adducts

**Figure 7.** Silver coordination in the Lewis acid base adducts $(\text{L})_x\text{AgAl}(\text{OR})_4$; $\text{R} = \text{C}(\text{H})(\text{CF}_3)_2$ or $\text{C}(\text{CH}_3)(\text{CF}_3)_2$.

$(\text{L})\text{AgAl}(\text{hftp})_4$ and $(\text{L})\text{AgAl}(\text{hftb})_4$ [$\text{hftb} = \text{OC}(\text{CH}_3)(\text{CF}_3)_2$], that is, $\text{L} = \text{toluene}$, CH_2Cl_2 , 1,2- $\text{Cl}_2\text{C}_2\text{H}_4$, S_8 , P_4 , and P_4S_3 .^{11–13} A common structural feature of these complexes is that the silver ion is coordinated by two oxygen atoms of the anion as schematically shown in Figure 7.

Clearly the strengths of the Ag–O coordination to the anion are a measure for the strengths of the interaction to the coordinated Lewis base L. The shorter is the Ag–O distance, the lower is the SIA to the Lewis base which leaves the silver ion more electrophilic. Long Ag–O separations are an indication for a strong SIA to the ligand L. A measure for the strength of the Ag–O interaction is the average Ag–O distance; however, less ambiguous³⁶ is the sum of the Ag–O bond valences s calculated according to I. D. Brown's bond valence method.³⁷ All structural data and bond valences s are collected in Table 3.

(34) (a) Ho, Y.-P.; Yang, Y.-C.; Klippenstein, S. J.; Dunbar, R. C. *J. Phys. Chem. A* **1997**, *101*, 3338 and references therein. (b) Guo, B. C.; Castleman, A. W. *Chem. Phys. Lett.* **1991**, *181*, 16. (c) Deng, H.; Kebabian, P. *J. Phys. Chem. A* **1998**, *102*, 571.

(35) (a) Ma, N. L. *Chem. Phys. Lett.* **1998**, *297*, 230. (b) Bauschlicher, C. W., Jr.; Partridge, H.; Langhoff, S. R. *J. Phys. Chem.* **1992**, *96*, 3273 and references therein. (c) Chatteraj, P. K.; Schleyer, P. v. R. *J. Am. Chem. Soc.* **1994**, *116*, 1067. (d) Ritze, H. H.; Radloff, W. *Chem. Phys. Lett.* **1996**, *250*, 415.

A comparison of the similar structural parameters of the Ag–P₄ complexes of the Al(hfip)₄[−] and Al(hftb)₄[−] anions in Table 3 shows that both have virtually the same basicity, and therefore both can be used to establish a solid-state SIA scale. On the basis of the strengths *s* of the Ag–O contacts in Table 3, the affinity of the ligand L to the silver ion increases according to P₄ < CH₂Cl₂ < P₄S₃ < S₈ < 1,2-C₂H₄Cl₂ < toluene.³⁸ This leveling is in good agreement with our observation that the Ag–P₄ complexes were only accessible in pentane or CS₂ solution^{12b} but not from CH₂Cl₂. In contrast, the Ag(S₈) complexes were also prepared from CHCl₃ or CH₂Cl₂.¹³

Conclusion

The Ag–P₄S₃ complexes in **1** and **2** are the first polymeric Lewis acid base adducts of AgAl(OR)₄ which prior always led to isolated molecular (OR = hfip) or isolated salt structures (OR = pftb). Currently, we examine the possible one-dimensional electric and silver ion conductivity of **1** and **2** (cf. copper halide adducts in refs 8, 9). The coordination chemistry of ternary mixtures AgAl(OR)₄/P₄S₃/L is an interesting perspective with a possible extension to supramolecular chemistry. These ternary mixtures should lead to larger but isolated purely inorganic supramolecular arrays which include six- or eight-membered rings as in **2** (Figure 3) as building blocks and in which the free coordination sites of the silver ion are saturated by the third ligand L, that is, S₈ or P₄. Synthetic efforts in this direction are on the way.

The exclusive but flexible η¹ coordination of all P₄S₃ cage atoms shows that the electronic structure of P₄S₃ is different to that of *tetrahedro*-P₄; P₄ includes no sterically active lone pair orbitals as shown by the η² coordination to the silver ion of the Al(OR)₄[−] anions.¹² In contrast, P₄S₃ has sterically active lone pair orbitals on all atoms. Although incorporating a cyclo P₃ unit similar to P₄, molecular P₄S₃ prefers η¹ coordination.

- (36) An ordering according to the average Ag–O bond lengths implies a linear relation between the bond energy and the bond lengths. It is known that the bond energy and bond lengths relation is better described by an exponential decrease of the bond energy with increasing bond lengths. This is included in I. D. Brown's bond valence method,³⁷ and therefore the ordering based on the sum of the Ag–O bond valences is more reliable.
- (37) The contacts *s* (in valency units vu) have been defined as $s = (R/R_0)^{-N}$, where *R* is the observed distance, *R*₀ is the covalent bond distance (bond order = 1) of the bond in question, and *N* is an empirically derived constant. For Ag(I)-O contacts, *N* = 7.4 and *R*₀ = 1.946 Å, see: Brown, I. D. In *Structure and Bonding in Crystals*; O'Keefe, M., Navrotsky, A., Eds.; Academic Press: London, 1981; Vol. 2, p 1.
- (38) However, in the 1,2-Cl₂C₂H₄ and toluene cases, two ligands L are bound to the silver ion, and one could argue that these two structures should be excluded. We decided to leave them in the scale since the coordination of the second ligand L reflects the high affinity of the silver ion to the ligand L. It may be understood as a predissociation that finally leads to the Ag-(L)₂⁺ cation and the Al(hfip)₄[−] anion (as always found with the less basic Al(pftb)₄[−] anion), which again is induced by the high affinity of L towards the silver ion.

Moreover, **1** and **2** include the first example of the long sought^{2b} sulfur coordination which had been postulated³⁹ but was not structurally verified. This flexible S or P coordination is the starting point for the frequently observed further degradation of the P₄S₃ molecule. Presumably, η¹ P₄S₃ rearranges intermediately to a η² complex, and then the transition metal fragments insert into the P–P (as in {IrCl(CO)(P₄S₃)(PPh₃)₂}⁴⁰) or P–S bond as in [cp₄Cr₄(CO)₉(P₄S₃)]^{7a} (with further rearrangement). The observed redistribution^{7a} of the P and S atoms of P₄S₃ upon reaction with transition metal fragments may be due to the facile exchange of a P–S single bond for a P=S double bond as in the bond-no-bond-structure **C** in Figure 3 above. On the basis of the strengths *s* of the Ag–O contacts of several (L)AgAl(OR)₄ complexes, the affinity of the ligand L to the silver ion increases according to P₄ < CH₂Cl₂ < P₄S₃ < S₈ < 1,2-C₂H₄Cl₂ < toluene.

Experimental Details

All manipulations were performed using standard Schlenk or drybox techniques in an atmosphere of purified dinitrogen or argon (H₂O and O₂ < 1 ppm). All solvents were rigorously dried by standard procedures, distilled, degassed prior to use, and stored under N₂. NMR spectra were recorded on a Bruker AC250 spectrometer and referenced against the solvent (¹H, ¹³C) or external aqueous AlCl₃ (²⁷Al) and 85% H₃PO₄ (³¹P). Raman spectra were recorded at room temperature on a Bruker IFS 66v spectrometer equipped with the Raman module FRA106 in sealed NMR tubes or melting point capillaries (1064 nm radiation, 2 cm^{−1} resolution). Elemental analyses were performed by the analytical laboratory of the institute.

Acknowledgment. We thank Prof. H. Schnöckel for valuable discussions and advice, and Dipl. Chem. G. Stöber for recording the Raman spectra of **1** and **2**. Financial support from the German science foundation DFG and the Fonds der Chemischen Industrie is gratefully acknowledged. This paper is dedicated to Prof. Dieter Fenske, in Karlsruhe, Germany, on the occasion of his 60th birthday.

Supporting Information Available: Full ellipsoid plots of **1** and **2** including the anions and individual structural parameters, drawings of the disorder in **1ab**, X-ray crystallographic files in CIF format, and full tables of the experimental anion Raman bands as well as the calculated (AgP₄S₃)₂²⁺ vibrational modes (PDF). This material is available free of charge via the Internet at <http://pubs.acs.org>.

JA012760V

- (39) Riess, J. G. *ACS Symp. Ser.* **1983**, 232, 17.
(40) Ghilardi, C. A.; Midollini, S.; Orlandini, A. *Angew. Chem.* **1983**, 95, 800; *Angew. Chem., Int. Ed. Engl.* **1983**, 22, 790.